

Chiral order emergence driven by quenched disorder

Coraline Letouze,¹ Pascal Viot,^{1,*} and Laura Messio^{1,†}

¹*Sorbonne Université, CNRS, Laboratoire de Physique Théorique de la Matière Condensée (LPTMC), F-75005 Paris, France*

(Dated: April 21, 2025)

Quenched disorder is expected to destroy order, such as when a random field is applied in a 2-dimensional magnetic system. Even when order exists in the presence of disorder, it is usually only the survival of the order of the clean model. We present here a surprising phenomenon where an order, driven by quenched disorder, emerges, that has nothing in common with the order present in the clean model. It's a new type of *order by disorder* that differs from the usual thermal or quantum one. The classical Heisenberg model on the $J_1 - J_3$ kagome lattice is studied by parallel tempering Monte Carlo simulations, with magnetic site vacancies. After analyzing the effect of a few impurities on the ground state, favoring non-coplanar configurations, we show the emergence of a low-temperature chiral phase and the progressive destruction of the collinear $q = 4$ Potts order, the only order present in the clean system.

In frustrated two-dimensional magnets with continuous spins, discrete symmetries can be broken and lead to finite temperature phase transitions: time-reversal or lattice symmetry breaking induce chirality, stripe orders or valence bond crystals[1, 2]. Quenched disorder is expected to destroy or weaken such emerging order. However, on the classical kagome spin model with first and third neighbor Heisenberg exchanges ($J_1 J_3$ HK), we show that site disorder not only breaks the discrete K_4 order of the pure system[3], but also brings about the appearance of a completely new chiral order (see Fig. 1). This phenomenon could turn out to be quite general, and is the consequence of two pieces that had previously been discovered but not assembled: i) Disorder can be the origin of order, as in the well-known case of thermal and quantum fluctuations[4], ii) Holes in a spin lattice favor the least-collinear configurations[5, 6].

In most cases the broken symmetries in a clean system can be determined from the set of ground states. When they are not all related by a symmetry of the Hamiltonian, we speak from accidental degeneracies, as in the case of classical spin liquids[7]. At finite temperature, entropic effects favor the subset of ground states with the highest density of low-energy excitations. This is called the thermal order by disorder (ObD) phenomena, which also occurs in its quantum version at zero temperature for finite spin values due to quantum fluctuations.

The kagome antiferromagnet is the paradigmatic model of ObD, embodied by the $S = 1/2$ compound Herbertsmithite[8], where both thermal and quantum fluctuations select coplanar states among its extensive number of ground states[9–11]. Among the many other kagome compounds (Kapellasite[12], Volborthite[13], Haydeite[14, 15], Sr-Vesignieite[16]...), Ba-Vesignieite $\text{BaCu}_3\text{V}_2\text{O}_8(\text{OH})_2$ [17–21] can be described by a classical spin model which also presents ObD, where we now study the effect of site dilution.

This $J_1 J_3$ HK model has ferromagnetic Heisenberg interactions J_1 between nearest neighbors and significant antiferromagnetic ones J_3 between third neighbors[22]

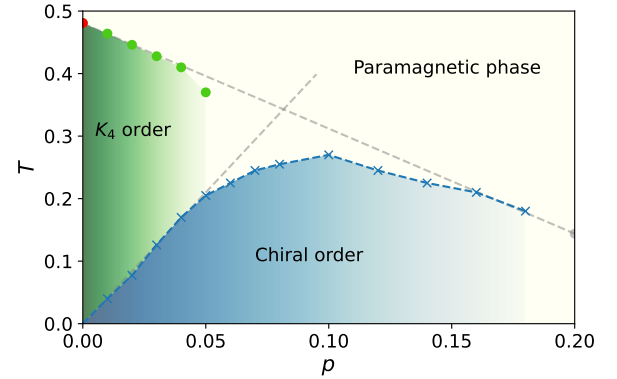


FIG. 1. Phase diagram of the $J_1 J_3$ HK model for $J_1 = -1$ and $J_3 = 1$. p is the rate of magnetic vacancies, T is the temperature. In the blue region the chirality $\chi \neq 0$. In the green region the Potts parameter $\sigma \neq 0$. The dots and crosses indicate phase transitions.

(see Fig. 2), with a Curie-Weiss temperature of about -77K :

$$\mathcal{H} = J_1 \sum_{\langle i,j \rangle} \eta_i \eta_j \mathbf{S}_i \cdot \mathbf{S}_j + J_3 \sum_{\langle i,j \rangle_3} \eta_i \eta_j \mathbf{S}_i \cdot \mathbf{S}_j, \quad (1)$$

where \mathbf{S}_i are 3d unit vectors, η_i is equal to 1 for a magnetic site and 0 for a non-magnetic site (vacancy). The η_i are statistically independent (uncorrelated disorder). $p = 1 - \sum_i \eta_i / N$ is the dilution parameter, with N the total number of sites. Site dilution is an example of quenched disorder. We recall that a phase transition in spin model with quenched disorder usually falls into one of the following two categories, depending on the order parameter and on the type of quenched disorder[23]: (i) *random field disorder*, which arises when the disorder lifts the degeneracy between different ordered states, explicitly breaking the symmetry. As a consequence of the Imry-Ma argument [24], this prevents long-range order in dimension $d \leq 2$, (ii) *random T_c disorder*, which preserves the broken-symmetry phase, but introduces spa-

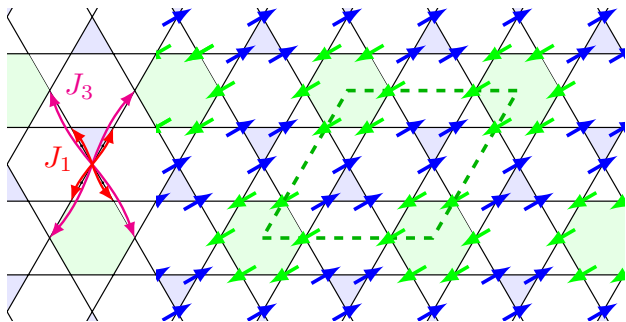


FIG. 2. Left: J_1 and J_3 interactions considered in the J_1J_3 HK model. Right: collinear K_4 order, with its unit cell represented by a dashed line.

tial variations in the critical temperature. According to the Aizenman-Wehr argument[25], a phase transition can still occur if the pure model satisfies $\nu d < 2$, where ν is the correlation length exponent $\xi \sim |T - T_c|^{-\nu}$. A representative example of these two categories is the $J_1 - J_2$ Ising model on the square lattice, where site dilution affects the low-temperature phases (which depend on the values of J_1 and J_2) differently. While it preserves the ferromagnetic phase (acting as a random T_c disorder), it destroys the stripe phase (acting as a random field disorder), by inducing a local breaking of the C_4 rotational lattice symmetry[23, 26, 27].

Theoretical studies of the pure J_1J_3 HK model have revealed a complex phase diagram[3, 28]. For $J_1 = 0$, the lattice decouples into three independent square sublattices, each exhibiting either ferromagnetic ($J_3 < 0$) or antiferromagnetic ($J_3 > 0$) order, leading in a 3-sublattice (for $J_3 < 0$) or 6-sublattice order (for $J_3 > 0$) (see Fig. 3). Beyond the expected $O(3)$ global spin rotational symmetry, an additional accidental degeneracy exists. When $J_3 > 0$, this accidental degeneracy is not lifted by a small J_1 (whatever its sign). The ground state manifold is called the 3subAF phase (see Fig. 3). By setting $J_3 = 1$, the range of J_1 values where this phase survives is quite extended[3]: $-1.24 \simeq -\frac{1+\sqrt{5}}{4} < J_1 < 1$. We fix the value of $J_3 = 1$ from now on. However, the aforementioned ObD lifts this degeneracy at low temperature, stabilizing a discrete collinear K_4 (or equivalently $q = 4$ Potts) order. The emergence of such a discrete order parameter in two dimensions via ObD has been observed in other models, such as the XY or Heisenberg $J_1 - J_2$ square lattice[29, 30], where two columnar states are selected from the ground state manifold, leading to a \mathbb{Z}_2 order. A similar phenomenon was recently reported in the $J_1 - J_2 - J_3$ square lattice[31] with an analogous K_4 symmetry breaking.

Inevitably, perturbations - such as spin anisotropies - are present in realistic systems and can lift the ground state degeneracy, potentially favoring phases with alternative broken symmetries. However, the K_4 phase of the

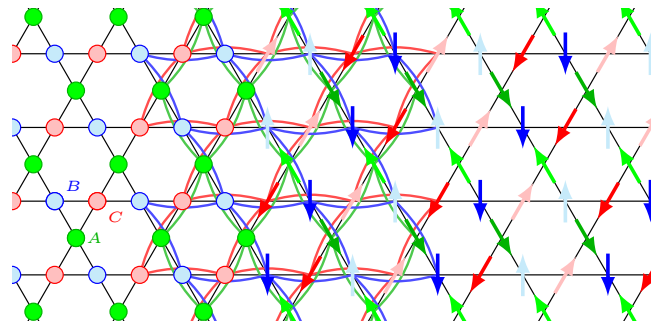


FIG. 3. Spin orientation in the 3subAF phase on the kagome lattice. Circles indicates the three sublattices A , B and C , related by the J_3 interaction (red, blue and green links). On each of the sublattices, spins have two opposite orientations, forming three independently oriented Néel orders. When all spins are collinear, we get the order of Fig. 2.

J_1J_3 HK can persist at moderate temperatures if its entropy advantage compensates the energy cost. We focus here on a specific perturbation: quenched disorder, which can induce unexpected effects[5, 32, 33], that are fundamentally different from uniform perturbations of the Hamiltonian. In the J_1J_3 HK model, it occurs that a discrete order parameter, chirality, emerges from site disorder, because it favors non-collinear configurations. The time-reversal symmetry is broken at low temperature, leading to a finite temperature phase transition. This reveals an unexpected result: a chiral ordered phase arising from quenched disorder, which is fundamentally different from the K_4 phase stabilized by entropic effects. Importantly, this phenomenon differs from a mere symmetry reduction that selectively eliminates certain ground states[27].

We present the phenomena selecting non-collinear configurations and then the numerical results evidencing the transition. Each configuration in the 3subAF phase is fully characterized by 3 spin orientations ($\mathbf{S}_A, \mathbf{S}_B, \mathbf{S}_C$) on a reference triangle ABC of the lattice, as it allows to propagate these orientations and their opposites on the whole lattice (Fig. 3). Global spin rotation are symmetries of the model, thus ground states related by such transformations are considered as equivalent (this continuous symmetry is only broken at $T = 0$ according to the Mermin Wagner theorem). The equivalence class of a ground state is thus specified by a couple ($\boldsymbol{\sigma}, \chi$) of a three dimensional real vector $\boldsymbol{\sigma}$ and a chirality $\chi = \pm 1$ defined on a triangle ABC as:

$$\boldsymbol{\sigma}_{ABC} = \begin{pmatrix} \mathbf{S}_B \cdot \mathbf{S}_C \\ \mathbf{S}_C \cdot \mathbf{S}_A \\ \mathbf{S}_A \cdot \mathbf{S}_B \end{pmatrix}, \quad \chi_{ABC} = \mathbf{S}_A \cdot (\mathbf{S}_B \wedge \mathbf{S}_C). \quad (2)$$

Among these classes, 4 have collinear spins $\pm \mathbf{S}_A = \pm \mathbf{S}_B = \pm \mathbf{S}_C$ resulting in 4 possible values for $\boldsymbol{\sigma}$ and

$\chi = 0$ (represented on Fig. 2 right) and 2 others have orthogonal spins pointing to the vertices of an octahedron ($\sigma = \mathbf{0}$ and $\chi = \pm 1$). The configurations with orthogonal spins are called octahedral. These two chiral spin states (among all other chiral ones) have the particularity to not break any lattice symmetry[34].

At low temperature and for $p = 0$, the 4 collinear classes of the 3subAF states are favored through thermal ObD[3]. It induces a discrete symmetry breaking related to the choice of one of the four possible classes (emergent $q = 4$ Potts, or K_4 order parameter). The order parameter for this order is denoted Σ and is defined in [3], while the chiral order parameter is χ : the average of χ_{ABC} over the lattice. Finite-size analysis have shown that the critical exponents are compatible with the 4 state Potts model universality class[3].

What are now the effect of a non-zero (small) p in the $J_1 J_3$ HK ? And first of all, does the K_4 order survive such disorder ? A random field coupled to a discrete order parameter is expected to destroy it in $d \leq 2$. In our case, although the disorder at hand is not a random field but site disorder, it still generates an effective random field, because both the K_4 order and the site vacancies break the translational lattice symmetries[23]. To illustrate this, we evaluate the effect of a small number of vacancies on the collinear spin configuration of Fig. 2 in the approximation where the state does not reorder to minimize its energy. It happens that a hole on a hexagon of green sites has the same energetic effect as a hole on a triangle of blue sites. However, as soon as two neighboring sites are empty, the energy difference with respect to the fully occupied state depends on the hole position: $8J_3 - J_1$ for two sites of different colors versus $8J_3 + J_1$ for two identical-color sites. Site disorder thus affects the 4 translationally equivalent collinear orders differently, similar to what a random field does on otherwise equivalent magnetizations. Thus, the K_4 order is expected to be killed by an infinitesimal $p > 0$. We will see that this seductive scenario is challenged by the numerical simulations.

Whatever, the competition between the 4 collinear states becomes completely irrelevant at very low temperature, as the energy minimization near vacancies kills any spin collinearity and allows the emergence of a new discrete order parameter, related to the chirality sign. Unlike K_4 , chirality does not break any lattice symmetry and does not suffer from any random field effect, fully allowing a phase transition in the presence of site disorder. To illustrate this, we begin by considering a single vacancy on a B -site of the kagome lattice (Fig. 3). For $J_1 = 0$, the presence or absence of this spin has strictly no effect on the ground state manifold, but switching on J_1 lifts the degeneracy. The A and C spins of the four first neighbors of the impurity experience an apparent magnetic field of length J_1 , in the direction opposite to the missing spin[35]. In a Néel antiferromag-

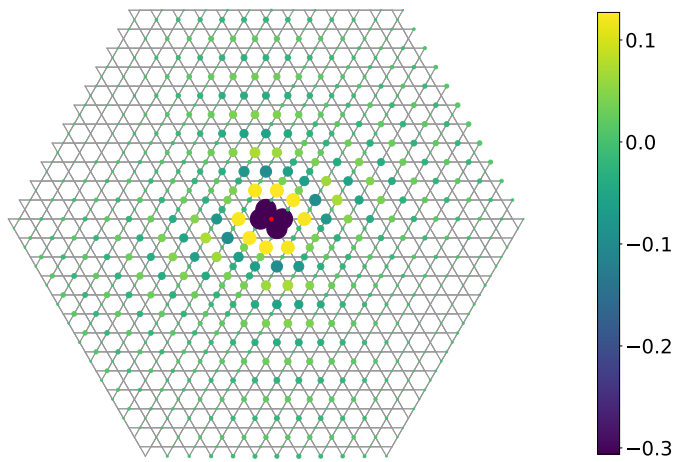


FIG. 4. Ground state spin-spin correlation $\mathbf{S}_i \cdot \mathbf{S}_0$ between sites i of the A and C sublattices and the central site 0 belonging to the B sublattice. The exchanges of the J_1 and J_3 links emanating from site 0 tend to zero. Correlations between B sites are not shown (they are strongly antiferromagnetic and near ± 1).

net, parallel and perpendicular magnetic susceptibilities differ: $\mathcal{S}_{\parallel} = 0$ while $\mathcal{S}_{\perp} > 0$: the spins tend to orient perpendicularly to the magnetic field and to minimize their energy by a canting that decreases when moving away from the impurity. As a consequence, the A and C Néel ordered sub-lattices orient quasi-perpendicularly to the B spins, with angles depending on the distance to the impurity (see correlations on Fig. 4) and alternating signs, similarly to Friedel oscillations already evidenced in other continuous spin models with single vacancies[36]. This phenomena is similar to the selection of the least-collinear order[5, 6], also observed on the $J_1 - J_2$ square model[27, 37, 38], explained by an effective positive bi-quadratic interaction $(\mathbf{S}_i \cdot \mathbf{S}_j)^2$ between neighboring spins. However, with a unique impurity, the A and C quasi-Néel orders remain mutually independent and we still expect them to align collinearly at infinitesimal temperatures, a partial survival of the initial thermal ObD. With one impurity, we have only two perpendicular spin directions, which is not enough to specify a chirality. On the $J_1 - J_2$ square lattice, the only 2 intricate Néel order prevent the apparition of chirality[38]. Here, with 3 sublattices and with vacancies on all types of sites, the 3 Néel orders tend to orient mutually perpendicularly, allowing to determine a local spin triad with definite chirality.

We performed extensive Monte Carlo simulations for site dilution $0 \leq p \leq 0.2$ and linear system size L from 24 to 128 (the number of sites is $N = 3L^2$). To minimize relaxation times, which can be significant at low temperatures, we employed a parallel tempering method combined with a local update provided by the heat bath algorithm [39]. Our numerical study focuses on the exchange parameters $J_1 = -1$ and $J_3 = 1$ (we also investigated

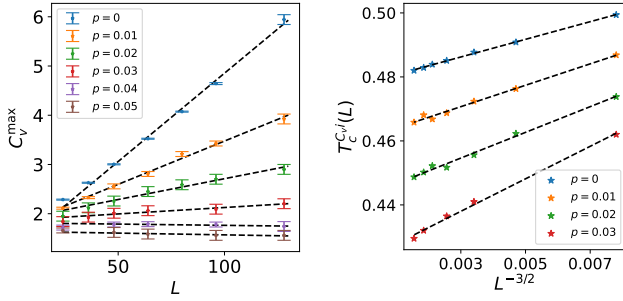


FIG. 5. (left) Maxima of heat capacity C_V^{\max} versus the linear lattice size L and (right) $T_c^{C_V}(L)$ versus $L^{-3/2}$, for several dilution rates p .

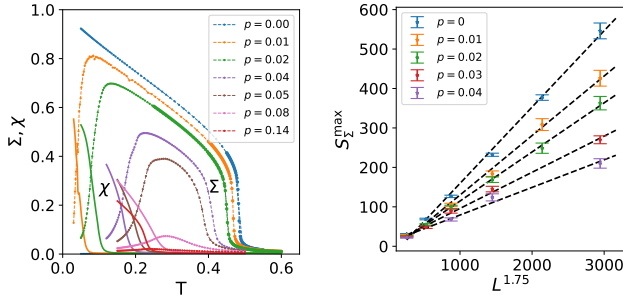


FIG. 6. (left) Order parameter Σ (increasing and decreasing with T) and χ (immediately decreasing) versus T for different dilutions and $L = 96$. (right) Maximum of the susceptibility S_X^{\max} versus $L^{1.75}$. The dotted lines correspond to linear fits.

$J_1 = -1.2$, resulting in a similar phase diagram[40]). For each L , simulations were performed with a minimum average of 10 disorder realizations.

The phase diagram $T - p$ is displayed in Fig. 1: the red dot at $p = 0$ corresponds to the already known phase transition of the pure model, belonging to the universality class of the 4-state Potts model[3] (with critical exponents verifying $\alpha/\nu = 1$, $\gamma/\nu = 7/4$, and $1/\nu = 3/2$), as clearly shown by finite-size scaling analysis (FSSA). We use the following relations for the maxima of the specific heat C_V and of the (connected) susceptibility S_X of the order parameter X (with $X = \Sigma$ or χ) to determine the nature of the phase transitions[41]:

$$\begin{aligned} C_V^{\max}(L) &= \frac{\overline{\langle \mathcal{H}^2 \rangle} - \overline{\langle \mathcal{H} \rangle}^2}{NT^2} \simeq aL^{\alpha/\nu} + b, \\ S_X^{\max}(L) &= \frac{\overline{\langle X^2 \rangle} - \overline{\langle X \rangle}^2}{NT} \simeq cL^{\gamma/\nu} + d, \\ T_c^Y(L) &\simeq eL^{-1/\nu} + T_c(\infty), \end{aligned} \quad (3)$$

where brackets denote thermal averages and overlines are averages over disorder realizations. T_c^Y is the temperature of the maximum of Y , where Y is C_V , Σ or χ .

We now discuss the phase diagram for $p \neq 0$. For low impurity rate $p < 0.05$, the transition temperature

between the paramagnetic phase and the K_4 order decreases rapidly with increasing p . We observe a linear dependence of $C_V^{\max}(L)$ (Fig. 5 left), but the amplitude a decreases rapidly with p . The evolution of $T_c^{C_V}(L)$ (Fig. 5 right) confirms that $\nu = 2/3$. Lastly, the maximum of the K_4 susceptibility S_Σ^{\max} increases as $L^{7/4}$ with a slope decreasing with p (Fig. 6 right). Thus FSSA clearly indicates that there is a phase transition in the same universality class as the pure model, i.e as the 4-state Potts model. This result seems to invalidate the argument that site dilution leads to the existence of local random fields, but we want to draw attention on the fact that other studies report transitions in presence of random fields, arguing that their lattice-symmetry breaking effect is very small[26].

At lower temperatures, a second phase transition appears, where we observe simultaneously a rapid decrease of Σ (K_4 order) and a rapid increase of χ (chiral order) as T decreases (see Fig. 6 left). In the presence of site disorder, non-collinear configurations are energetically favored, overcoming the entropic advantage of the K_4 order at very low temperatures. The thermodynamic signature of this transition is the appearance of a small secondary maximum in C_V at $T_c \simeq 4p$ for $p < 0.05$, which increases weakly with L (e.g., $C_V^{\max}(28) = 1.15$, $C_V^{\max}(128) = 1.20$). This prevents the determination of a reliable scaling exponent with FSSA, that however remains compatible with the scaling of the dilute Ising spin model[42]. S_χ appears to be weakly dependent on the system size L , while S_Σ follows a scaling behavior with an exponent slightly larger than 1. To obtain stable results in this regime, a disorder average over 20 realizations is required. Results are also limited to $L \leq 80$, due to thermalization difficulties.

For $0.05 \leq p \leq 0.1$, Σ collapses to zero at all temperatures as L increases. This behavior becomes more pronounced as p increases[40]. In the thermodynamic limit, we expect the K_4 order to vanish, which may indicate that site dilution finally acts as a random field and kills the transition for $p > 0.05$. At low temperatures, the chiral order is present below a critical temperature that increases with the dilution, but saturates at $p \simeq 0.1$ (see Fig. 1). For $0.1 \leq p \leq 0.2$, the K_4 order is clearly absent, and the chiral order weakens as p increases with a progressive decrease of the critical temperature. Nevertheless, one observes a significant versatility of behaviors: for $p = [0.14, 0.16]$, C_V displays a small but noticeable divergence with the system size[40]. Moreover, the maximum of S_χ still diverges with L , even though its value decreases due to the site dilution, which isolates some of the complete triangles where χ is defined. FSSA unveils that this maximum scales as $L^{1.7}$ which is compatible with the Ising universality class.

For $p = 0.2$, the chiral order parameter collapses with L , which can be interpreted as the absence of a phase transition due to disorder overcoming some percolation

threshold. On the kagome lattice, triangles form a honeycomb lattice and have a probability of $(1-p)^3$ to be fully occupied by magnetic sites. Equating in a crude approximation this value with the site percolation threshold of the honeycomb lattice (equal to 0.697[43]) gives a critical dilution $p_c = 0.11$, but this has to be taken with care as further neighbor interactions complicate this view in term of percolation.

In summary, we have shown on the example of the J_1J_3 HK model with magnetic site vacancies that quenched disorder can lead to the emergence of a specific order (here chiral), that was forbidden in the clean phase (with collinear K_4 order). This phenomenon can be designated as the *order by quench disorder* mechanism that differs from the usual thermal or quantum order by disorder. Although this expression has been previously employed[6], our proposal is distinct in that it involves the breaking of time-reversal symmetry in the absence of a magnetic field and in contrast to the pure model. A similar birth of chirality is expected for other models such as the triangular or honeycomb lattices with stripe orders[34, 44], due to the lattice decoupling in more than two sublattices (similar to what occurs in the J_1J_3 HK model). The exploration of classical spin liquids[7] represents another direction for further research on order from quenched disorder.

ACKNOWLEDGMENTS

L.M thanks Eric Andrade for invaluable discussions on the effect of disorder, and the IIT Madras for its hospitality that made these discussions possible.

* pascal.viot@sorbonne-universite.fr

† laura.messio@sorbonne-universite.fr

- [1] M. Hasenbusch, A. Pelissetto, and E. Vicari, Critical behavior of two-dimensional fully frustrated XY systems, *Journal of Physics: Conference Series* **42**, 124 (2006).
- [2] J.-C. Dornier, C. Lhuillier, L. Messio, L. Pierre, and P. Viot, Chirality and \mathbb{Z}_2 vortices in a Heisenberg spin model on the kagome lattice, *Phys. Rev. B* **77**, 172413 (2008).
- [3] V. Grison, P. Viot, B. Bernu, and L. Messio, Emergent Potts order in the kagome $J_1 - J_3$ Heisenberg model, *Phys. Rev. B* **102**, 214424 (2020).
- [4] Villain, J., Bidaux, R., Carton, J.-P., and Conte, R., Order as an effect of disorder, *J. Phys. France* **41**, 1263 (1980).
- [5] V. S. Maryasin and M. E. Zhitomirsky, Triangular antiferromagnet with nonmagnetic impurities, *Phys. Rev. Lett.* **111**, 247201 (2013).
- [6] A. I. Smirnov, T. A. Soldatov, O. A. Petrenko, A. Takata, T. Kida, M. Hagiwara, A. Y. Shapiro, and M. E. Zhitomirsky, Order by quenched disorder in the model triangular antiferromagnet $\text{RbFe}(\text{moo}_4)_2$, *Phys. Rev. Lett.* **119**, 047204 (2017).
- [7] H. Yan, O. Benton, R. Moessner, and A. H. Nevidomskyy, Classification of classical spin liquids: Typology and resulting landscape, *Phys. Rev. B* **110**, L020402 (2024).
- [8] M. A. de Vries, J. R. Stewart, P. P. Deen, J. O. Piatek, G. J. Nilsen, H. M. Rønnow, and A. Harrison, Scale-free antiferromagnetic fluctuations in the $s = 1/2$ kagome antiferromagnet herbertsmithite, *Phys. Rev. Lett.* **103**, 237201 (2009).
- [9] J. T. Chalker, P. C. W. Holdsworth, and E. F. Shender, Hidden order in a frustrated system: Properties of the Heisenberg kagomé antiferromagnet, *Phys. Rev. Lett.* **68**, 855 (1992).
- [10] R. Moessner and J. T. Chalker, Low-temperature properties of classical geometrically frustrated antiferromagnets, *Phys. Rev. B* **58**, 12049 (1998).
- [11] M. E. Zhitomirsky, Octupolar ordering of classical kagome antiferromagnets in two and three dimensions, *Phys. Rev. B* **78**, 094423 (2008).
- [12] B. Fåk, E. Kermarrec, L. Messio, B. Bernu, C. Lhuillier, F. Bert, P. Mendels, B. Koteswararao, F. Bouquet, J. Ollivier, A. D. Hillier, A. Amato, R. H. Colman, and A. S. Wills, Kapellasite: A Kagome Quantum Spin Liquid with Competing Interactions, *Phys. Rev. Lett.* **109**, 037208 (2012).
- [13] Z. Hiroi, H. Yoshida, Y. Okamoto, and M. Takigawa, Spin-1/2 kagome compounds: Volborthite vs Herbertsmithite, *J. Phys.: Conf. Ser.* **145**, 012002 (2009).
- [14] R. Colman, A. Sinclair, and A. Wills, Comparisons between Haydeite, $\alpha\text{-Cu}_3\text{Mg}(\text{OD})_6\text{Cl}_2$, and Kapellasite, $\alpha\text{-Cu}_3\text{Zn}(\text{OD})_6\text{Cl}_2$, Isostructural $S = 1/2$ Kagome Magnets, *Chem. Mater.* **22**, 5774 (2010).
- [15] R. H. Colman, A. Sinclair, and A. S. Wills, Magnetic and Crystallographic Studies of Mg-Herbertsmithite, $\gamma\text{-Cu}_3\text{Mg}(\text{OH})_6\text{Cl}_2$ —A New $S = 1/2$ Kagome Magnet and Candidate Spin Liquid, *Chem. Mater.* **23**, 1811 (2011).
- [16] A. Verrier, F. Bert, J. M. Parent, M. El-Amine, J. C. Orain, D. Boldrin, A. S. Wills, P. Mendels, and J. A. Quilliam, Canted antiferromagnetic order in the kagome material Sr-vesignieite, *Phys. Rev. B* **101**, 054425 (2020).
- [17] Y. Okamoto, H. Yoshida, and Z. Hiroi, Vesignieite $\text{BaCu}_3\text{V}_2\text{O}_8(\text{OH})_2$ as a Candidate Spin-1/2 Kagome Antiferromagnet, *J. Phys. Soc. Jpn.* **78**, 033701 (2009).
- [18] H. Yoshida, Y. Michiue, E. Takayama-Muromachi, and M. Isobe, Vesignieite $\text{BaCu}_3\text{V}_2\text{O}_8(\text{OH})_2$: a structurally perfect $S = 1/2$ kagomé antiferromagnet, *J. Mater. Chem.* **22**, 18793 (2012).
- [19] Y. Okamoto, M. Tokunaga, H. Yoshida, A. Matsuo, K. Kindo, and Z. Hiroi, Magnetization plateaus of the spin-1/2 kagome antiferromagnets volborthite and vesignieite, *Phys. Rev. B* **83**, 180407 (2011).
- [20] H. Ishikawa, T. Yajima, A. Miyake, M. Tokunaga, A. Matsuo, K. Kindo, and Z. Hiroi, Topochemical Crystal Transformation from a Distorted to a Nearly Perfect Kagome Cuprate, *Chem. Mater.* **29**, 6719 (2017).
- [21] R. H. Colman, F. Bert, D. Boldrin, A. D. Hillier, P. Manuel, P. Mendels, and A. S. Wills, Spin dynamics in the $S = \frac{1}{2}$ quantum kagome compound vesignieite, $\text{Cu}_3\text{Ba}(\text{VO}_5\text{H})_2$, *Phys. Rev. B* **83**, 180416 (2011).
- [22] D. Boldrin, B. Fåk, E. Canévet, J. Ollivier, H. C. Walker, P. Manuel, D. D. Khalyavin, and A. S. Wills, Vesignieite: An $S = \frac{1}{2}$ Kagome Antiferromagnet with Dom-

- inant Third-Neighbor Exchange, *Phys. Rev. Lett.* **121**, 107203 (2018).
- [23] T. Vojta, Disorder in quantum many-body systems, *Annual Review of Condensed Matter Physics* **10**, 233 (2019), <https://doi.org/10.1146/annurev-conmatphys-031218-013433>.
- [24] Y. Imry and S.-k. Ma, Random-field instability of the ordered state of continuous symmetry, *Phys. Rev. Lett.* **35**, 1399 (1975).
- [25] M. Aizenman and J. Wehr, Rounding of first-order phase transitions in systems with quenched disorder, *Phys. Rev. Lett.* **62**, 2503 (1989).
- [26] S. S. Kunwar, A. Sen, T. Vojta, and R. Narayanan, Tuning a random-field mechanism in a frustrated magnet, *Phys. Rev. B* **98**, 024206 (2018).
- [27] X. Ye, R. Narayanan, and T. Vojta, Stripe order, impurities, and symmetry breaking in a diluted frustrated magnet, *Phys. Rev. B* **105**, 024201 (2022).
- [28] H. Li and T. Li, Competing emergent Potts orders and possible nematic spin liquids in the kagome J_1-J_3 Heisenberg model, *Phys. Rev. B* **106**, 035112 (2022).
- [29] C. L. Henley, Ordering due to disorder in a frustrated vector antiferromagnet, *Phys. Rev. Lett.* **62**, 2056 (1989).
- [30] P. Chandra, P. Coleman, and A. I. Larkin, Ising transition in frustrated Heisenberg models, *Phys. Rev. Lett.* **64**, 88 (1990).
- [31] M. G. Gonzalez, A. Fancelli, H. Yan, and J. Reuther, Magnetic properties of the spiral spin liquid and surrounding phases in the square lattice XY model, *Phys. Rev. B* **110**, 085106 (2024).
- [32] A. Andreanov and P. A. McClarty, Order induced by dilution in pyrochlore XY antiferromagnets, *Phys. Rev. B* **91**, 064401 (2015).
- [33] E. Shender, V. Cherepanov, P. Holdsworth, and A. Berlinsky, The kagome Antiferromagnet with defects: satisfaction, frustration and spin folding in a random spin System, *Phys. Rev. Lett.* **70**, 3812 (1993).
- [34] L. Messio, C. Lhuillier, and G. Misguich, Lattice symmetries and regular magnetic orders in classical frustrated antiferromagnets, *Phys. Rev. B* **83**, 184401 (2011).
- [35] C. L. Henley, Effective hamiltonians and dilution effects in kagome and related anti-ferromagnets, *Canadian Journal of Physics* **79**, 1307 (2001), <https://doi.org/10.1139/p01-097>.
- [36] P. M. C onsoli and M. Vojta, Disorder effects in spiral spin liquids: Long-range spin textures, friedel-like oscillations, and spiral spin glasses, *Phys. Rev. B* **109**, 064423 (2024).
- [37] M. M. J. Miranda, I. C. Almeida, E. C. Andrade, and J. A. Hoyos, Phase diagram of a frustrated Heisenberg model: From disorder to order and back again, *Phys. Rev. B* **104**, 054201 (2021).
- [38] C. Weber and F. Mila, Anticollinear magnetic order induced by impurities in the frustrated Heisenberg model of pnictides, *Phys. Rev. B* **86**, 184432 (2012).
- [39] Y. Miyatake, M. Yamamoto, J. J. Kim, M. Toyonaga, and O. Nagai, On the implementation of the 'heat bath' algorithms for Monte Carlo simulations of classical Heisenberg spin systems, *J. Phys. C: Solid State Phys.* **19**, 2539 (1986).
- [40] Supplemental material.
- [41] H. Rieger and A. P. Young, Critical exponents of the three-dimensional random field Ising model, *Journal of Physics A: Mathematical and General* **26**, 5279 (1993).
- [42] V. S. Dotsenko and V. S. Dotsenko, Critical behaviour of the phase transition in the 2d Ising model with impurities, *Advances in Physics* , 129 (1983).
- [43] J. L. Jacobsen, High-precision percolation thresholds and Potts-model critical manifolds from graph polynomials, *Journal of Physics A: Mathematical and Theoretical* **47**, 135001 (2014).
- [44] A. Mulder, R. Ganesh, L. Capriotti, and A. Paramekanti, Spiral order by disorder and lattice nematic order in a frustrated Heisenberg antiferromagnet on the honeycomb lattice, *Phys. Rev. B* **81**, 214419 (2010).

Supplemental Material to Chiral order emergence driven by quenched disorder

Coraline Letouze,¹ Pascal Viot,¹ and Laura Messio¹

¹*Sorbonne Université, CNRS, Laboratoire de Physique Théorique de la Matière Condensée (LPTMC), F-75005 Paris, France*

(Dated: April 21, 2025)

Simulation results for the $J_1 - J_3$ model are presented in detail for different dilutions p , within the phase diagram of the J_1J_3 HK model. For small p , a finite-temperature transition is observed between the paramagnetic phase and the 4-state Potts (K_4) ordered phase, with the critical temperature decreasing linearly with dilution. At low temperatures, a second transition occurs, where the K_4 order disappears and is replaced by chiral order. For $p > 0.05$, the K_4 order vanishes, and at low temperature, the chiral order is associated with a continuous transition. The critical exponents appear to be compatible with an Ising-type transition. For $p > 0.2$, the chiral order also disappears.

We distinguish 3 regimes: small, moderate and large dilution, according to the changes in the nature of phase transitions, together with the $p = 0$ pure case, and visualized on Fig. 1 for $J_3 = 1$ and $J_1 = -1$.

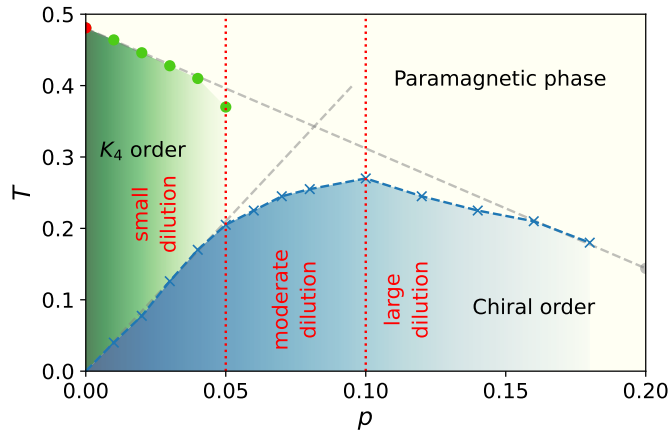


FIG. 1. Phase diagram of J_1J_3KH model with $J_3 = 1$ and $J_1 = -1$, presented in the main article.

The curves presented for each regime are obtained from several temperature runs performed in parallel, with the parallel tempering method, which regularly attempts exchanges between consecutive temperatures. The two order parameters that are measured are defined in the main article and are

- Σ , associated to a broken K_4 symmetry (or equivalently $q = 4$ Potts order),
- and χ , the chirality associated to broken time reversal symmetry and non-coplanarity of the configuration.

For each of order parameter X , the connected susceptibility S_X is also evaluated using the average of Σ^2 and χ^2 for each disorder realisation (formula in the main article).

The linear size L of the lattice is related to the number of kagome sites N via $N = 3L^2$.

I. PURE MODEL

The pure model ($p = 0$) exhibits a finite-temperature phase transition already detailed in [1], where both the specific heat C_V and the susceptibility S_Σ diverge with L (see Fig. 2). Finite-size scaling analysis indicates that the critical exponents are consistent with those of the bidimensional four-state Potts model, as expected. Simulations were conducted for different lattice sizes, $L = 24, \dots, 128$. Figure 2 shows the evolution of C_V , Σ , and S_Σ . We also performed simulations at low temperature ($T = 0.05$), but the chirality χ remains always close to zero, which confirms that the order-by-disorder (ObD) mechanism only involves the Σ order parameter.

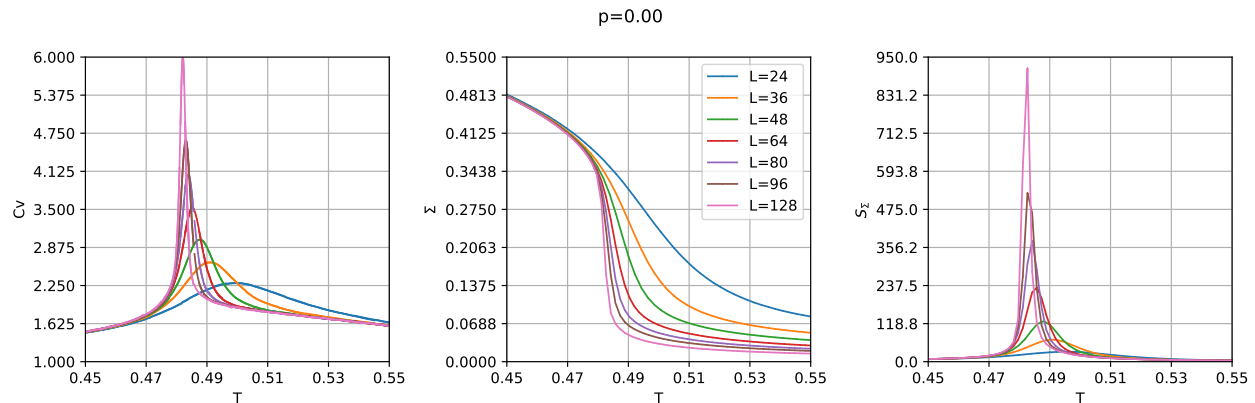


FIG. 2. (From left to right) Heat capacity C_V , K_4 order parameter Σ , chiral susceptibility S_χ for the pure model ($p = 0$).

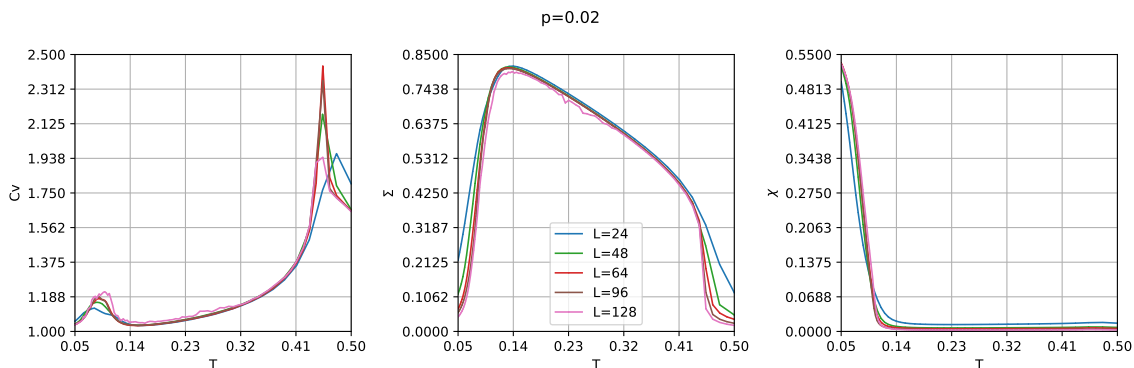


FIG. 3. From left to right: heat capacity C_V , order parameters Σ and χ for $p = 0.02$.

II. SMALL DILUTION

We consider the small dilution region ($0 < p < 0.05$). Fig. 3 and 4 present the simulation results respectively for $p = 0.02$ and $p = 0.03$ and for different system sizes L .

Fig. 3 shows C_V , Σ , and χ versus T for $p = 0.02$. Two successive phase transitions occur for decreasing temperatures in this range of dilutions, corresponding to the two peaks in C_V :

- At high temperatures ($T \simeq 0.45$), the first transition corresponds to the emergence of K_4 order, while the chiral order parameter χ remains zero. Note that the critical temperature is lower than for the pure model ($T_c(p=0) = 0.48$).
- At lower temperatures ($T \simeq 0.08$), a second transition occurs, marked by a sudden drop in Σ to a small value, accompanied by a rapid increase in χ .

Fig. 4 illustrates again these two successive phase transitions for a slightly larger $p = 0.03$, but focuses separately on the high and low-temperature regions.

The high- T plots show C_V , Σ and the susceptibility S_Σ as functions of T for different system sizes L . Finite-size scaling analysis indicates that this transition belongs to the same universality class as the pure K_4 model (see scaling results in the main text).

The low- T plots show C_V , Σ and χ and highlight the low-temperature phase transition. Here, C_V shows little variation with the system size. Near the transition, Σ decreases significantly when T decreases, while the chiral order parameter χ — initially zero — increases rapidly.

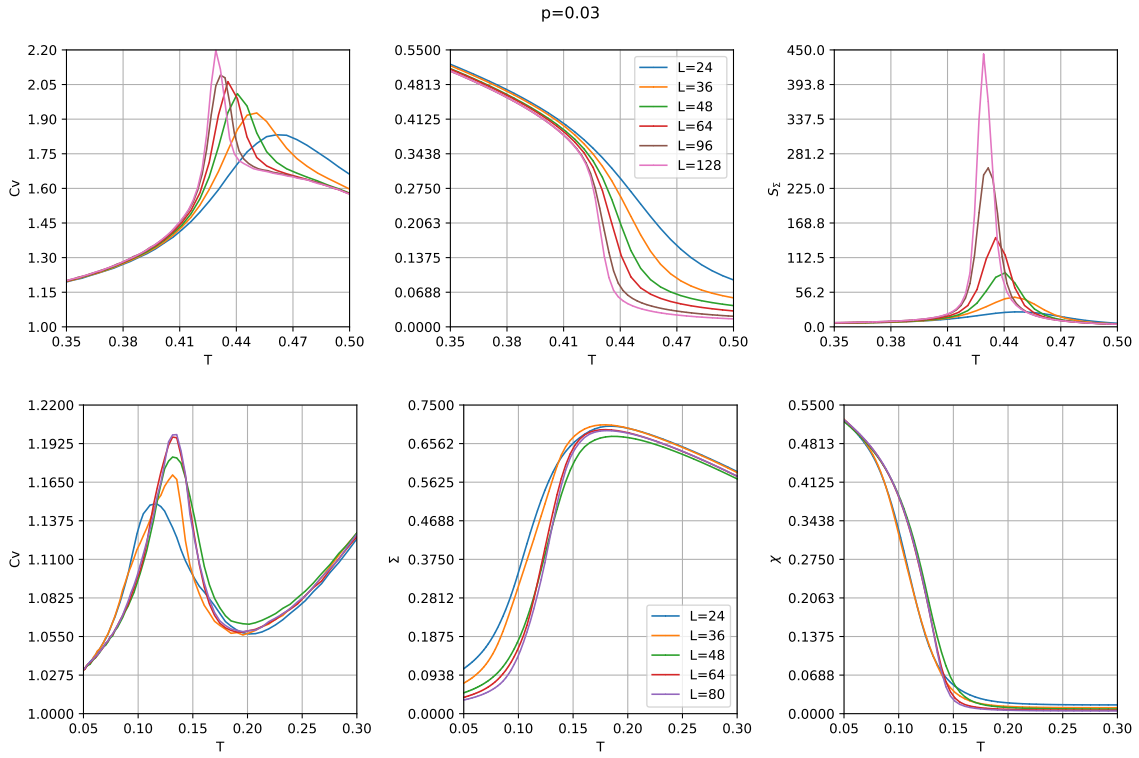


FIG. 4. Results for $p = 0.03$. Top: C_V , Σ and S_Σ versus T near the high-temperature phase transition, bottom: C_V , Σ and χ for T near the low-temperature phase transition.

III. MODERATE DILUTION

For $0.05 \leq p \leq 0.1$, Σ tends to zero for any temperature as L increases, suggesting that the Potts order does not survive in the thermodynamic limit. The example of $p = 0.07$ is given in Fig. 5. The low- T peak of C_V disappears, leaving only a shoulder. However, the susceptibility S_χ continues to diverge with an exponent yet to be determined (not shown).

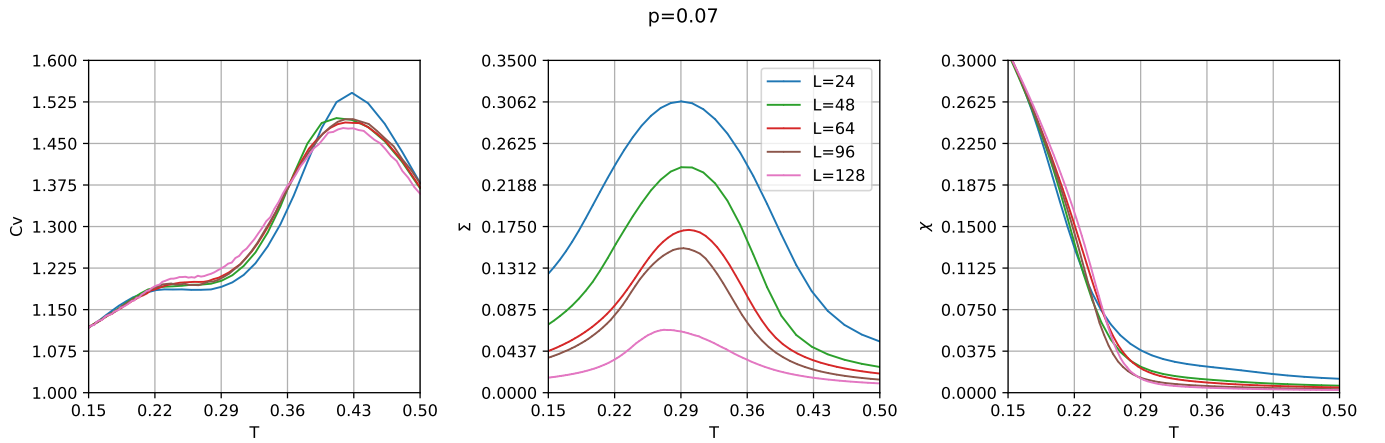


FIG. 5. (From left to right) C_V , Σ and χ for $p = 0.07$.

IV. "LARGE" DILUTION

For $0.1 < p < 0.2$, the situation becomes simpler. Fig. 6 shows the evolution of C_V , χ , and the susceptibility S_χ versus T for different lattice sizes L . The transition is now more clearly identified by a maximum in C_V that increases with L , even if the evolution is quite slow.

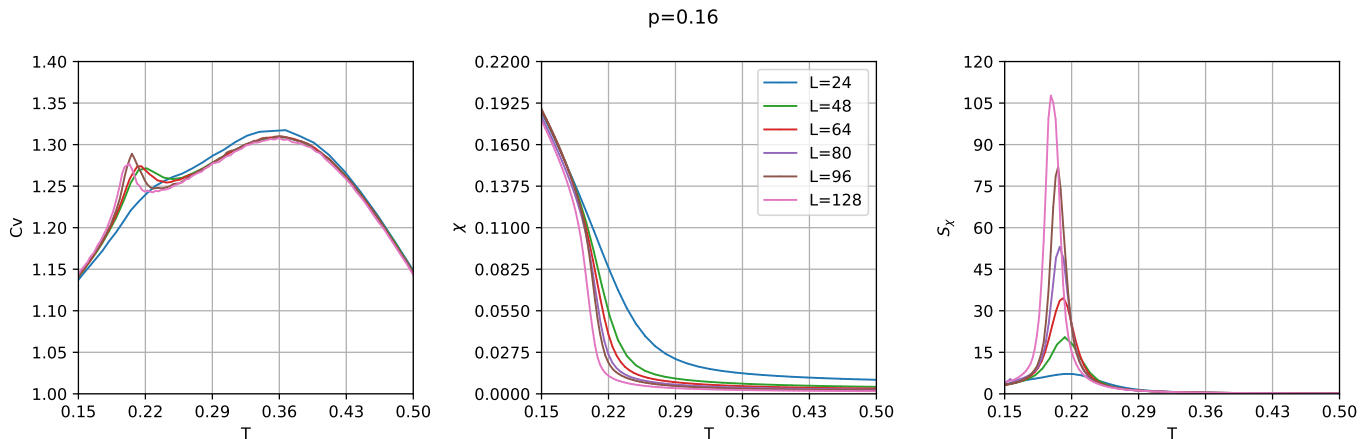


FIG. 6. (From left to right) Heat capacity C_V , chiral order parameter χ , and the susceptibility S_χ for $p = 0.16$.

Moreover, in this region, the chiral transition occurs at a temperature that decreases with dilution. Since the chiral order resides on triangles that are free of site dilution, the density of available triangles decreases rapidly with p . To determine the universality of the transition, we consider the maximum of the chiral susceptibility S_χ , which, as expected, exhibits a power-law behavior with an exponent consistent with an Ising transition (see Fig. 7).

When p increases, the intensity of the order parameter diminishes. Finally, simulations for $p \geq 0.2$ lead to a chiral order parameter that decreases with the system size. This behavior can be interpreted as related to some percolation property for the triangles with three occupied sites (but the exchanges between first and third neighbors complicate this picture).

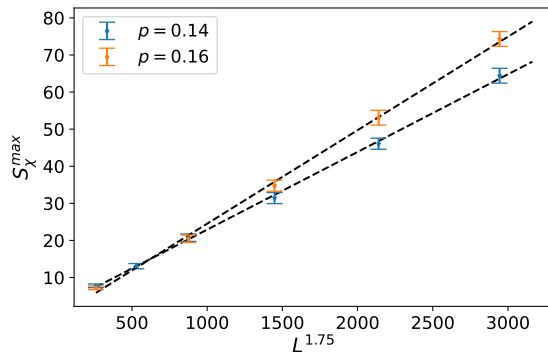


FIG. 7. S_χ^{max} versus the linear size L for two dilutions $p = 0.14, 0.16$

V. PHASE DIAGRAM OF THE $J_1 J_3$ HK MODEL WITH $J_1 = -1.2$

In all previous results, we have chosen $J_3 = 1$ and $J_1 = -1$. In order to enlarge our study, we now consider the effect of disorder when the ferromagnetic coupling is larger $J_1 = -1.2$.

For the pure model, the critical temperature is shifted to a higher value compared to the pure model with $J_1 = -1$. By introducing increasing disorder dilution, one obtains a very similar phase diagram, with the same universality classes for each region (see Fig. 8).

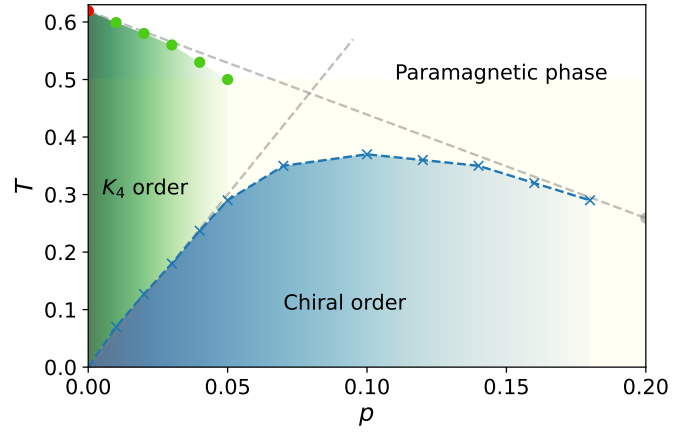


FIG. 8. Phase diagram of J_1J_3KH model with $J_3 = 1$ and $J_1 = -1.2$.

The numerical simulations were performed on the LPTMC-LKB-LJP cluster, during approximately 40000d.core, equivalent to 2800kg eq.CO₂, using the approximate rate of 3.6g.core⁻¹.h⁻¹[2].

-
- [1] V. Grison, P. Viot, B. Bernu, and L. Messio, Emergent Potts order in the kagome $J_1 - J_3$ Heisenberg model, *Phys. Rev. B* **102**, 214424 (2020).
- [2] F. Berthoud, B. Bzeznik, N. Gibelin, M. Laurens, C. Bonamy, M. Morel, and X. Schwindenhammer, *Estimation de l'empreinte carbone d'une heure.coeur de calcul*, Research Report (UGA - Université Grenoble Alpes ; CNRS ; INP Grenoble ; INRIA, 2020).